The simulation and interpretation of free turbulence with a cognitive neural system

Francesc Giralt[a)]
Departament d'Enginyeria Química, Universitat Rovira i Virgili, Carretera de Salou s/n, 43006 Tarragona, Catalunya, Spain

A. Arenas, J. Ferre-Giné, and R. Rallo
Departament d'Enginyeria Informàtica, Universitat Rovira i Virgili, Carretera de Salou s/n, 43006 Tarragona, Catalunya, Spain

G. A. Kopp[b)]
Departament d'Enginyeria Química, Universitat Rovira i Virgili, Carretera de Salou s/n, 43006 Tarragona, Catalunya, Spain

(Received 8 July 1999; accepted 15 March 2000)

An artificial neural network, based on fuzzy ARTMAP, that is capable of learning the basic nonlinear dynamics of a turbulent velocity field is presented. The neural system is capable of generating a detailed multipoint time record with the same structural characteristics and basic statistics as those of the original instantaneous velocity field used for training. The good performance of the proposed architecture is demonstrated by the generation of synthetic two-dimensional velocity data at eight different positions along the homogeneous (spanwise) direction in the far region ($x/D=420$) of a turbulent wake flow generated behind a cylinder at $\mathrm{Re}=1\,200$. The analysis of the synthetic velocity field, carried out with spectral techniques, POD and pattern recognition, reveals that the proposed neural system is capable of capturing the highly nonlinear dynamics of free turbulence and of reproducing the sequence of individual classes of relevant events present in turbulent wake flows. The trained neural system also yields patterns of the coherent structures embedded in the flow when presented with input data containing partial information of the instantaneous velocity maps of these events. In this way, the neural network is used as an expert system that helps in the structural interpretation of turbulence in a wake flow. [S1070-6631(00)00407-4]

I. INTRODUCTION

Turbulence is a fluid flow phenomenon of significant fundamental interest as well as of commercial importance for its impact on the operational performance and costs of many industrial processes, transportation systems and engineered structures (e.g., long-span bridges). It is characterized by an irregular space and time dependence of the velocity and scalar fields which is the result of vortical three-dimensional motions that occur at high Reynolds numbers, when the ratio of inertial to viscous forces is high.[1,2] Turbulence is an unsolved classical problem[3] so that the study of turbulent flows relies heavily on experimental data and, more recently, on the direct numerical solution of the Navier–Stokes equations of fluid motion. The interpretation and control of the very large range of excited space and time scales present in these flows, and of the associated mixing that they cause,[4] requires the application of analytical, experimental and computational techniques.[5]

It is now well known that there are large-scale, recurrent, coherent eddies among the vortical motions present in turbulent flows. The flow visualizations carried out by Brown and Roshko[6] and Falco[7] were among the first to show these motions. A large number of quantitative techniques, such as spatial correlation functions and POD,[8–10] pattern recognition and conditional averaging,[11–15] etc., have been used to determine or identify the structure of turbulent fields. The dynamic significance of these structures has been shown in a variety of turbulent flows.[16–19]

The techniques described above use features of the coherent motions to identify and educe them from the measured or numerical data sets, in a closed, noninteractive mode. Ferre-Giné *et al.*[14] developed a fuzzy-neural network pattern recognition technique which operates as an automatic classification technique, free from operator bias, capable of categorizing all types of coherent and disordered motions present in the data. This capability could be exploited to generate turbulent signals if the method were reversed. In other words, it could predict a sequence of classes of patterns from an initial velocity condition. Of course, such a simulation would only succeed if the artificial neural network had learned the nonlinear dynamics of the turbulent flow. If such a simulation did succeed, then it could also be possible to apply the system openly and interactively to identify the structure present in any turbulent flow as an expert system.

[a)]Telephone: +34-977559638; Fax: +34-977559621. Electronic mail: fgiralt@etseq.urv.es
[b)]Present address: Boundary Layer Wind Tunnel Laboratory, Faculty of Engineering Science, University of Western Ontario, London, ON, N6A 5B9, Canada.

Here we report a cognitive neural network architecture based on fuzzy ARTMAP[20] that is capable of learning the basic nonlinear dynamics of a turbulent velocity field and to generate, afterwards, a detailed multipoint time record, as detailed as can be measured in a laboratory experiment. The problem dealt with in the present study at the simulation stage is not that of exactly forecasting the measured field but that of generating the turbulent field after learning the basic statistics and structural characteristics from historic examples of the original.[21,22] At the interpretation or expert system stage, the trained neural system is used to determine the existence and topology of coherent structures that could be present in the flow field investigated. This is done by generating sequences of data from inputs containing partial information of the velocity field of the hypothesized structure. The flow analyzed is a fully developed turbulent wake generated by a circular cylinder.

II. THE NEURAL SYSTEM

A. Background and network requirements

An artificial neural network is a modeling and computational technique based on the observed behavior of biological neurons which is used to mimic the performance or simulate the dynamics of a system from examples. In some cases these networks are used in combination with the theory of fuzzy logic so that in addition to learning from experience, they can carry out tasks faster with less computer space requirements by accepting both numerical data and fuzzy commands as inputs. Fuzzy and neural systems, or a combination of the corresponding logic and network architectures, have been applied to identify, classify, control, forecast, predict, diagnose, model, design and analyze events in several fluid-base systems of interest to medicine, vehicle and transportation systems, aerospace, manufacturing, meteorology and mining.[23] Examples of fluid-base applications in engineering include the reduction of drag, the minimization of energy consumption or losses, the prediction of transport rates in industrial equipment, the reduction of noise, and phenomena related to pressure dynamics.

A significant portion of the above mentioned applications are related to flow turbulence and arise from the need to control some aspects of this highly nonlinear phenomenon. Thus, the performance of a neural system in these applications could be evaluated by its ability to learn the dynamics of turbulence in some pre-selected regions of the flow field. Feedforward, feedback, and other standard architectures are capable of capturing some aspects of the dynamics of turbulent flows. For example, Lee *et al.*[24] have established the correlation between some near-wall turbulence parameters and the wall actuation needed to reduce drag. However, it remains to be determined whether these or other architectures are capable of first learning and then simulating, in a global sense, flow turbulence.

One indispensable requirement for attempting the simulation of a synthetic turbulent velocity field (i.e., of simultaneous multipoint turbulent velocity time-records) with a neural network is that the architecture should be capable of learning the irregular time sequences of velocity patterns associated with turbulence. This requires that the artificial neural system should be able to select, in an automated way, a path in this complex sequence of real events or patterns on the basis of past experience. Therefore, it should:

(i) Be able to accurately classify patterns in difficult classification situations.

(ii) Be capable of generalizing incoming information with an efficient mechanism for resetting patterns and creating new categories. This will ensure avoidance of the stability-plasticity dilemma[20,25–27] of either hindering stability by endlessly activating new categories in competitive learning or by losing the plasticity or ability of the network to react to any new data because the learning rate is gradually reduced to zero. This characteristic of the Adaptive Resonance Theory (ART) is important in the real time learning of systems that are continuously adapting in a nonstationary situation. The more popular feedforward and feedback architectures present the difficulty of establishing the dimension of the system or number of neurons that are required for the network to exhibit long-time memory capabilities. A pertinent discussion on the long-time memory requirements to resolve ambiguities in forecasting problems can be found in Kühn *et al.*[28]

(iii) Have associative memory or memory organization accessed by its content, with a sufficiently long span to resolve the ambiguities in the succession states that characterize the dynamics of highly nonlinear systems. The architecture should remember by retrieving previously stored information in response to associated data.

(iv) Use fuzzy rules in the learning algorithm since they are especially useful in the treatment of real data.[29]

One reasonable choice which has the above characteristics is the Fuzzy ARTMAP neural system.

B. Architecture

The Fuzzy ARTMAP neural network is formed by a pair of fuzzy ART modules, Art_a and Art_b, linked by an associative memory and an internal controller.[20] This is sketched in Fig. 1 with the output disconnected.

The Fuzzy ART architecture was designed by Carpenter *et al.*[27] for multidimensional data clustering based on a set of features. The elements of the set of n-dimensional data vectors $\{\xi^1,\ldots,\xi^p\}$, where p is the number of vectors to be classified, must be interpreted as a pattern of values showing the extent to which each feature is present.

Every pattern must be normalized to satisfy the following conditions:

$$\xi^i \in [0,1]^n$$
$$\sum_{j=1}^{n} \xi_j^i = k \quad \forall i = 1,..,p. \tag{1}$$

The classification procedure of fuzzy ART is based on Fuzzy Set Theory.[30] The similarity between two vectors can

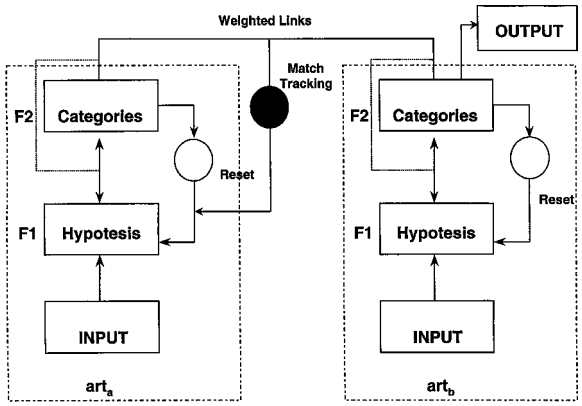

FIG. 1. Individual neural network architecture.

be established by the grade of the membership function, which for two generic vectors (l, m) can be easily calculated as

$$\text{grade}(\xi^l \subset \xi^m) = \frac{|\xi^l \wedge \xi^m|}{|\xi^l|}. \tag{2}$$

In Eq. (2) the fuzzy AND operator $\wedge$ is defined by

$$\wedge:[0,1]^n \times [0,1]^n \rightarrow [0,1]^n$$

while the components of the image vector that result from this application are

$$\xi_j^i = \min(\xi_j^l, \xi_j^m) \quad \forall j = 1,...,n. \tag{3}$$

The norm $|\bullet|$ in Eq. (2) is the sum of the components of the vector defined by Eq. (3).

The classification algorithm clusters the data that have a value of (2) greater than the *vigilance parameter* ρ into groups or classes. The value of ρ controls the granularity of the classes and allows the implementation of a desired accuracy criteria in the classification procedure. Each class μ is represented by a vector ω^μ, the weight vector. The procedure starts by creating the first class from the first pattern presented to the network

$$\omega^1 = \xi^1. \tag{4}$$

The rest of input patterns ξ^i $(i=2,...,p)$ are presented to the network and if the similarity of ξ^i with any established class μ is greater than ρ then ξ^i is classified into this class, and the representative of this class is updated according to

$$\omega_{\text{new}}^\mu = \omega_{\text{old}}^\mu \wedge \xi^i. \tag{5}$$

Otherwise a new class represented by ξ^i is created. Equation (5) is the learning rule of the net. The mechanisms to speed up the process and to conduct the classification properly can be found elsewhere.[27]

The dynamics of Fuzzy ARTMAP are essentially the same as two separate Fuzzy ART networks, each one working with a part of the training vector; the first part could be interpreted as the input pattern and the second one as the desired classification output (supervisor). The associative memory records the link between the classes corresponding to the input pattern and the desired classification. The internal controller is responsible for supervising if a new link is in contradiction with any other previously recorded. If no contradiction is found, the link is recorded, but in the case of a contradiction, the pattern is re-classified with a larger vigilance parameter. Once the network has been trained it can be used to classify input vectors without any additional information.

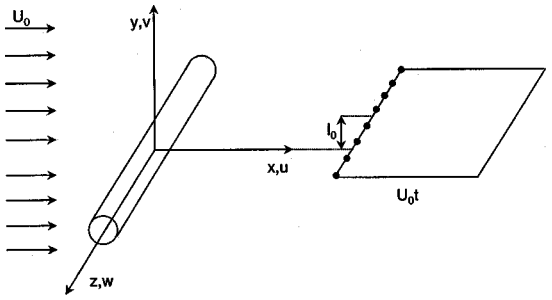

FIG. 2. Sketch of the flow configuration.

The Fuzzy ARTMAP architecture was designed to classify data and, thus, cannot generate an output pattern after the training stage. To implement this new mode of operation the categories educed by the system from the learned information are linked to the desired outputs, as depicted in Fig. 1. This is mathematically equivalent to defining a mapping from the space of categories to that of output patterns, the image of the mapping being defined by examples of patterns provided to the neural system in a supervised manner. The accuracy of the procedure increases asymptotically towards a constant value with the number of examples used for training, i.e., when the space of outputs is accurately mapped. In the predictive mode, only the category layer of Art_b in Fig. 1 is active and linked to Art_a to provide an output for each input vector presented to this module.

C. Experimental data and training sets

The performance of the proposed neural system has been evaluated by simulating the two-dimensional velocity field measured at eight different positions $(k=1,2,...,8)$ along the homogeneous (spanwise) direction of a turbulent wake flow generated behind a cylinder at $\text{Re}=1200$ and $x/D=420$. The freestream velocity of this flow was $U_0=6.7\,\text{m/s}$ and the cylinder diameter $D=2.67\,\text{mm}$. The structural characteristics of these fully developed turbulent wake data, provided by R. A. Antonia (University of Newcastle), have been previously examined by Kopp *et al.*[15] using pattern recognition and proper orthogonal decomposition (POD). Figure 2 illustrates the experimental flow configuration for the case where the (u, w) velocity data were measured with eight X-wire probes located along the homogeneous spanwise direction at the half width of the wake $(l_0=12.3\,\text{mm})$. Here, l_0 is the lateral (y) location where the mean velocity defect is half the maximum value. The eight sensors spanned approximately $2.87l_0$ in the z direction. The voltage signals were sampled at 2717 Hz for 30 s. Taylor's hypothesis was used to convert the time measurements into the spatial coordinate $x=-U_0t$ in all plots.

The neural system proposed was formed by eight Fuzzy ARTMAP networks like the one shown in Fig. 1. These

networks were working in parallel and synchronously, one for each experimental device measuring simultaneously the two-component velocity signals u and w at a given k-location in the wake flow. Each individual network was first trained with the output in Fig. 1 disconnected. The training data for each individual network consisted of vectors with 12 elements for the Art_a module, four temporal or historical velocity components (u and w) for the probe under consideration, plus the two components of the two spatially adjacent probes. Vectors with two elements, the following value of each velocity component in the time sequence, were used for the Art_b module. Thus, simultaneous space–time information was provided to the neural system in terms of the input to each Art_a module, with the corresponding future information for (u, w) given to each Art_b module, with no other association between individual networks. At the two extreme locations ($k=1$ and 8) the spatial information was provided from the one-sided contiguous locations ($k+1$, $k+2$) and ($k-1$, $k-2$), respectively.

The dimension of the input vectors to the eight neural networks and the type of simultaneous space–time information that they contained was decided after examination of the space–time correlation of the experimental data, so that relevant structural characteristics of the flow were provided to the system during training. The choice of four temporal data for each velocity component in the training input vector is consistent with Takens theorem.[31] This theorem states that good accuracy can be achieved in point-to-point forecasting in a system with attractors of dimension d when a function that depends at most on $(2d+1)$ past measurements is used. For the wake flow this implies using between four and five historical data in the training sets.

The system was trained using the first 2000 instants of the experimental velocity field (u, w). This was sufficient to match the local fractal dimension of 1.75 ± 0.02 and 1.78 ± 0.02 of the simulated u and w signals, respectively, with the values 1.76 ± 0.02 and 1.78 ± 0.02 of the experimental data. The local fractal dimension was calculated by the box-counting dimension procedure described by Scott *et al.*[32] Additional training tests with up to 40 000 samples yielded comparable statistics but improved structural characterization, as is discussed in the next section. A nonoptimized version of the code required less than 1 h of total CPU time for training in a Sun Ultra−2/300 workstation.

After training, instants (2001–2004) of measured u and w at each location were used together with the two spatial data of the instant 2004 as the initial input vector to the Art_a module of each net. The output (u, w) for the instant 2005 was generated by each Art_b module with only the categories layer and the output activated. The output calculated by each network was added to the corresponding data sequence and a new input pattern was formed with historicals (2002–2005) and with the two spatial data predicted simultaneously by the two neighboring networks also at instant 2005. Such operation of the neural system produced a two-component velocity field of eight velocity data pairs (u, w) every 0.14 s of CPU with the two processors of the workstation working in parallel.

III. SIMULATION OF FREE TURBULENCE

A. Statistics from the simulation

To evaluate the performance of the proposed network architecture 81 600 time instants (29.4 s) of (u, w) velocity signals were generated at time intervals of $\Delta t=0.368$ ms. No repetitions in the predicted velocity field were observed over this time-period. The (u, w) results obtained in the homogeneous x-z plane of the wake are evaluated in detail in this section using basic statistics, spectral and correlation analysis, POD and pattern recognition. The preliminary evaluation of the performance of the proposed neural system for non-homogeneous turbulence (x-y plane) is also reported. All space variables are normalized with respect to l_0 as

$$x^*=\frac{\Delta X}{l_0}\cong\frac{-U_0\Delta t}{l_0},\quad y^*=\frac{\Delta y}{l_0},\quad z^*=\frac{\Delta z}{l_0}.$$

The flow in all vector maps is from left to right. The statistics of the two-dimensional instantaneous turbulent velocity field (u, w) measured and simulated by the present architecture with training sets of 2000 and 24 000 samples labeled ANN-2000 and ANN-24 000, respectively, are given in Table I.

The comparison of the statistics of the two predicted time records shows that training with 2000 instants of data is sufficient to capture the irregularity of the time sequence, as is also the case for the local fractal dimension. Thus, the results analyzed in this section correspond mostly to ANN-2000. The mean of the predicted velocity field reported in Table I deviates a maximum of 0.2%, in terms of the free stream velocity, from the (zero mean) experimental fluctuating field. The rms (root-mean-square) values of the fluctuating field generated for u and w are also in agreement with experimental data, with a maximum deviation of 9.2%. The Reynolds shear stress field is equal to zero, within the limits of the experimental error of the data, as should be the case in the homogeneous spanwise direction of the wake.

The auto-spectra of the simulated data is in good accordance with the experiments for both velocity components at all spanwise locations, as illustrated by the spectra of u and w, shown in Fig. 3 at one of the eight spanwise locations studied. These spectral results indicate that the neural system captures the energy distribution of both signals up to frequencies of 1 kHz, i.e., in the frequency range where aliasing errors are negligible.

The spatial correlation for the experimental and simulated u velocity component is depicted in Fig. 4. Comparison between the correlation contours in both cases shows that the neural system resolves the flow field well up to a spanwise location $z^*=-0.2$, i.e., up to an extent of approximately five probes. The auto-correlation functions for the experimental and simulated data, observed along the x^*-direction at the top of Figs. 4(a) and 4(b) for the extreme probe at location $z^*=1.2$, are also in good agreement down to correlations of 0.10. The 0.05 level occurs at $x^*\cong\pm2.5$ in the simulated data, slightly shortening the streamwise correlation. Similar accordance is found between the spatial correlation of the experimental and simulated w velocity fields (not shown here for brevity).

TABLE I. Statistics of the experimental and simulated data with velocities in m/s.

	Experimental			ANN-2000			ANN-24000		
	mean	rms	uw	mean	rms	uw	mean	rms	uw
u_1	0.000	0.118		0.010	0.119		0.008	0.114	
w_1	0.000	0.087	0.001	−0.002	0.083	0.001	−0.001	0.081	0.001
u_2	0.000	0.117		0.012	0.109		0.004	0.108	
w_2	0.000	0.087	0.002	0.000	0.087	0.001	0.001	0.079	0.001
u_3	0.000	0.118		0.012	0.113		0.003	0.110	
w_3	0.000	0.087	0.000	0.001	0.080	0.000	−0.001	0.079	0.000
u_4	0.000	0.117		0.016	0.109		0.006	0.110	
w_4	0.000	0.087	0.000	−0.003	0.082	0.000	−0.000	0.078	0.000
u_5	0.000	0.120		0.009	0.109		0.004	0.113	
w_5	0.000	0.088	0.001	0.003	0.086	0.001	0.002	0.081	0.001
u_6	0.000	0.117		0.011	0.110		0.007	0.115	
w_6	0.000	0.088	0.000	0.011	0.085	0.000	0.003	0.077	0.001
u_7	0.000	0.120		0.010	0.120		0.005	0.117	
w_7	0.000	0.087	−0.001	0.007	0.082	−0.001	0.001	0.080	0.000
u_8	0.000	0.111		−0.007	0.108		0.002	0.106	
w_8	0.000	0.084	−0.002	−0.005	0.083	−0.002	−0.002	0.079	−0.001

B. Structure of the simulated data

An estimate of the overall flow structure for the experimental and simulated velocity flow fields is given in Figs. 5 and 6, via the first and second eigenvectors obtained from POD. The neural system adequately describes the flow structure of the turbulent wake flow as indicated by the good agreement observed in these plots between the measured and the simulated fields. The first eigenvector obtained from the simulated two-dimensional velocity field [Fig. 5(b)] projects to the one of the real data [Fig. 5(a)] with a correlation coefficient of 0.97. The neural system identifies the negative fluctuating velocity motions that dominate the wake flow,[14,15] as illustrated by the first eigenvector. This satisfactory description of structure is also observed in the second eigenvector [Figs. 6(a) and 6(b)]. In this case the neural system also captures the presence of saddle points in the wake flow. In both Figs. 5 and 6 there is a progressive randomization of the structure for negative z^*, consistent with the randomization of the correlation contours presented in Fig. 4.

A pattern recognition analysis, carried out to determine the large-scale structural characteristics of the simulated flow, shows that 765 windows of 44 instantaneous velocity data with double rollers and 714 windows with saddle points are contained in a simulated time-record of 81 600 instants. This compares favourably to the 922 and 895 windows of the respective structures present in the experimental data. The 11% reduction in the number of structures present in the simulated data may be due to the inability of the neural system to learn continuity or the three-dimensional structural characteristics from two-dimensional information or it may be due to the loss of correlation as discussed regarding Fig. 4. It should be mentioned that the proposed neural architecture learned mass conservation when it was applied to a two-dimensional isotropic turbulent velocity field.

The corresponding prototypical patterns or ensemble-averages of the double rollers and saddle points identified by pattern recognition are depicted in Figs. 7 and 8 for both the simulated and experimental velocity fields. The agreement in topology between both vector maps is reasonable, with the saddle point appearing upstream of the double roller in both cases. The correlation between the patterns in Figs. 7(a) and 7(b) and between those in Figs. 8(a) and 8(b) are 0.80 and 0.86, respectively. This performance is remarkable when it is considered that the 2000 instants of velocity information

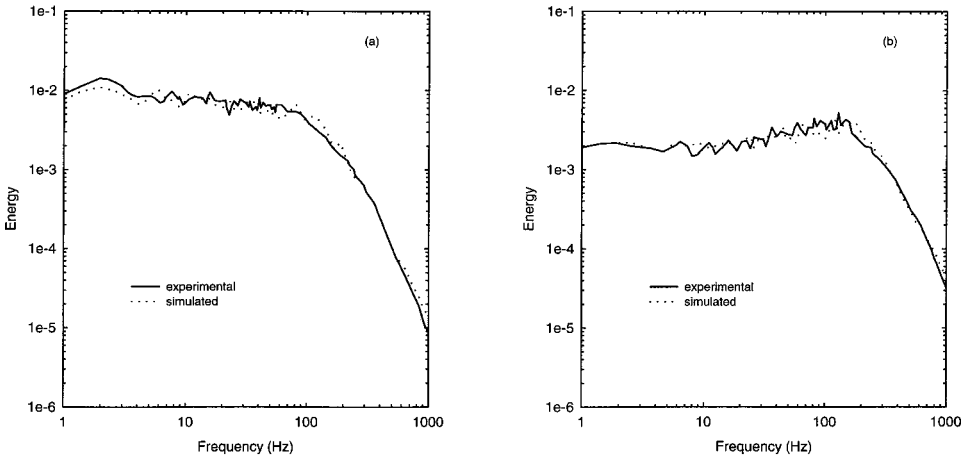

FIG. 3. Autospectra of the experimental and simulated (a) streamwise and (b) spanwise velocity components.

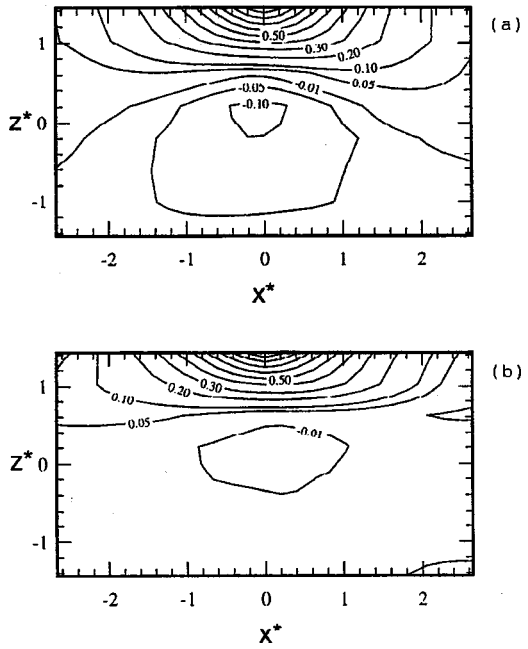

FIG. 4. Correlation of the streamwise velocity field from the (a) experimental and (b) simulated velocities.

used for training contain only about 22 structures. Note that the observed correlations increase to 0.94 when 40 000 instants are used for training, i.e., when the ANN-40000 is used to generate the time-record of 81 600 instants.

A similar performance of the neural system was obtained for data measured along the nonhomogeneous vertical plane

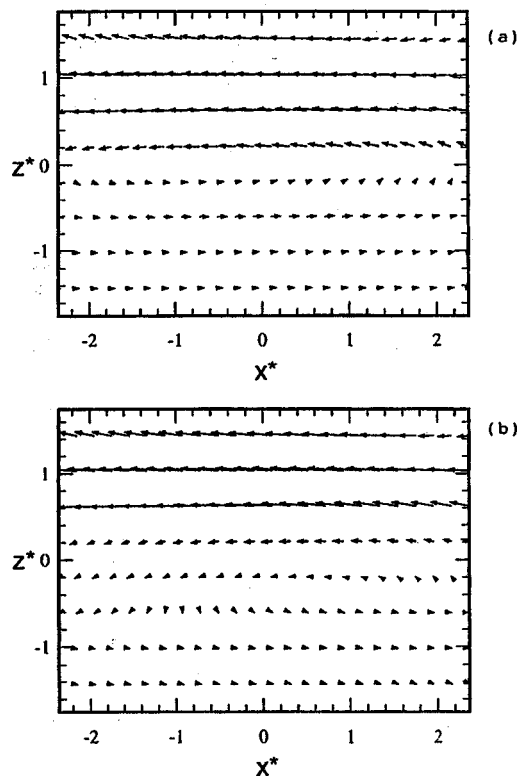

FIG. 5. First eigenvector from the POD analyses of the (a) experimental and (b) simulated data.

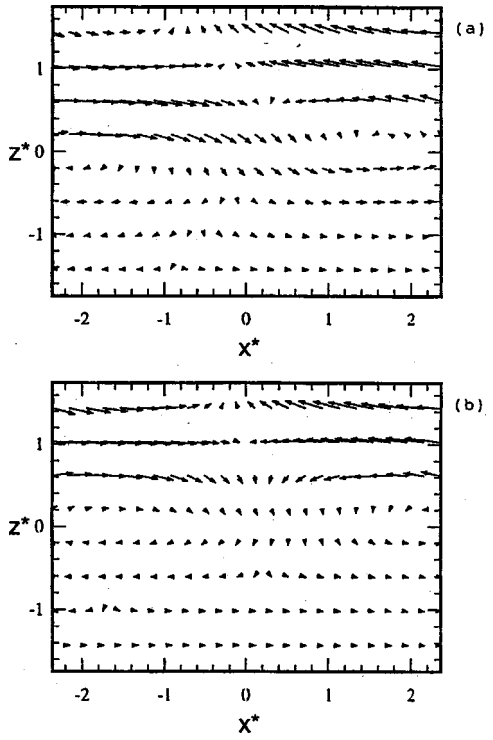

FIG. 6. Second eigenvector from the POD analyses of the (a) experimental and (b) simulated data.

of the wake (x^*-y^*). The rake of probes was centered at the wake centerplane $y^*=0$ and spanned vertically the whole wake. In this case, the number of classes contained in the signals measured at the eight different vertical positions depends on the different number of turbulent events sensed by the hot-wires located near the centerplane or near the outer edges of the wake. As a consequence of this depen-

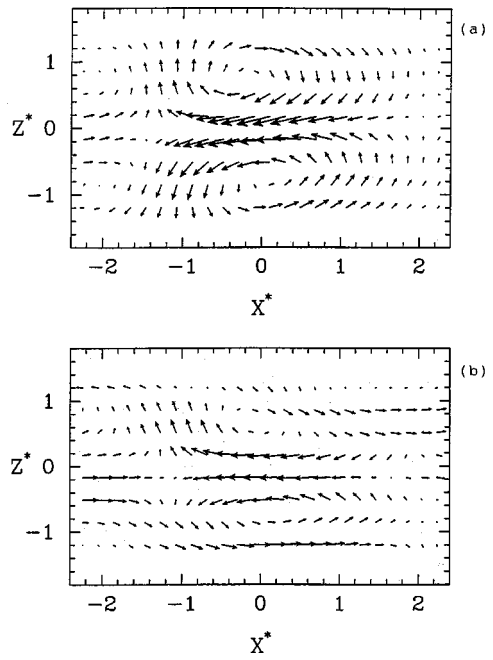

FIG. 7. Pattern recognition analyses of double rollers: (a) Experimental and (b) simulated data.

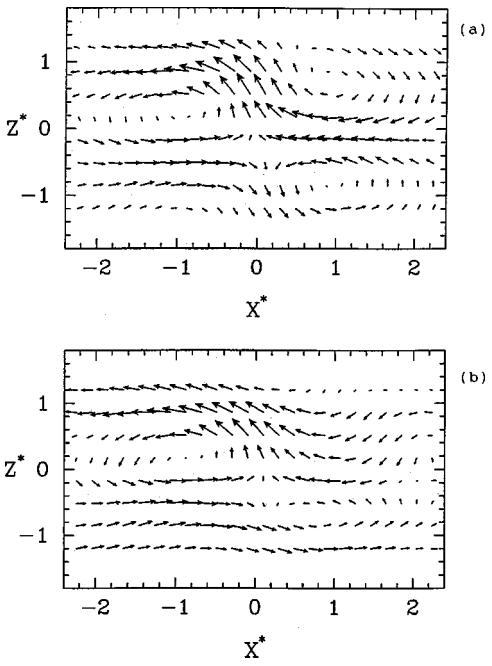

FIG. 8. Pattern recognition analyses of saddle points: (a) Experimental and (b) simulated data.

dency on intermittency, at least 6000 instants of the real velocity field (u, v) were needed to train the eight networks, and to capture enough information from the different velocity records so that the generated nonhomogeneous turbulent field reproduces the experimental one. It should be noted that the information contained in the vertical plane data is more difficult to learn by the neural system because the coherent structures and associated velocity patterns occurring at the outer edge are different from those at the center region of the wake. In the horizontal plane, homogeneity implies that the same type of information is ultimately presented to each individual network.

To assess the capability of the trained neural system to interpret the large-scale structure of a turbulent velocity field as an expert system it is necessary to first study whether or not the system is capable of generating instantaneous velocity patterns with the correct structural features of the flow analyzed. To investigate this, the 922 data windows contributing to the double roller ensemble-average of Fig. 7(a) were utilized. In particular, for each of these 922 windows, the four temporal points for each sensor at positions $0.4 \leqslant x^* \leqslant 1.0$ in Fig. 7(a) were used as the historical input to the neural system. The following 10 points of the time series (i.e., the positions $-1.5 \leqslant x^* \leqslant 0.4$ in Fig. 7(a) were generated for each sensor in exactly the same way as the simulation described above was performed. Figure 9 shows the ensemble average of these 922 simulated events. Note that these input data were not included in the training sets of ANN-2000. Clearly, the structure in Fig. 9 corresponds to the class of large-scale motions represented by the double roller in Fig. 7(a). This result indicates that with the same input information as that occurring instantaneously in a laboratory experiment, the neural system generates a group of instantaneous events that yield an ensemble average or prototypical pattern (Fig. 9) that also belongs to the class considered as the input [Fig. 7(a)].

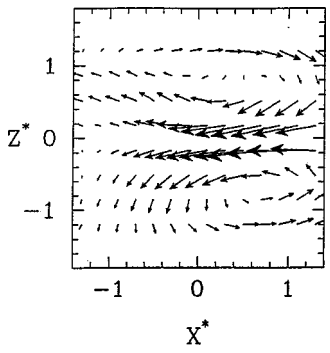

FIG. 9. Ensemble average of vectors maps predicted by the neural system when fed with input vectors of experimental data extracted from the instantaneous events that contribute to the double roller of Fig. 7 at positions $0.4 \leqslant x^* \leqslant 1.0$.

The architecture proposed is, thus, well suited to interpret free turbulence, as illustrated in the next section, and for real time applications involving turbulent flows. It can also be used to complete time sequences of important data that are limited in size due to difficulties in their acquisition or prediction. For example, the accurate direct numerical simulation of a turbulent flow requires intensive use of CPU time,[33] which for some flow situations or Reynolds numbers of interest may not be sufficiently available at present. Therefore, the synthetic generation of turbulent velocity or scalar signals or fields with a neural system may be a useful and complementary tool for computational fluid dynamics (CFD). It should be noted that the application of the proposed fuzzy ARTMAP architecture to DNS data would require different training and analysis due to the different spatial and time resolution of numerical calculations.

IV. INTERPRETATION OF TURBULENCE

The next step in the evaluation of the neural system is as an interactive expert system to help with the identification of the structural characteristics of turbulence in a flow not previously studied. To simplify this problem it will be assumed here that the unknown turbulent flow is the turbulent wake flow analyzed in the previous section.

A. Known characteristics

The challenge considered is to determine whether the presence of the double roller structure postulated more than forty years ago from correlation data[8,34] exists instantaneously in the flow learned by the neural system. Two interpretation experiments are considered:

(i) Education of a double roller with point-to-point forecasting from an sketch of an idealized or assumed template of this structure. (In point-to-point forecasting, the template ''data'' are always used for the four temporal or historical inputs.)

(ii) Testing for double rollers from a single input vector containing the initial portion of the above idealized template.

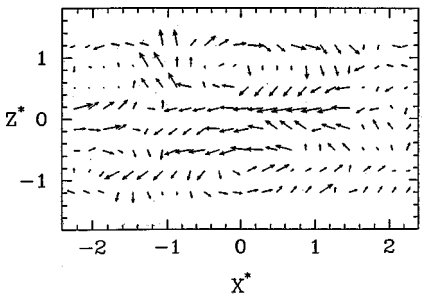

FIG. 10. Point-to-point forecasting of a vector map from an idealized and scaled double roller template.

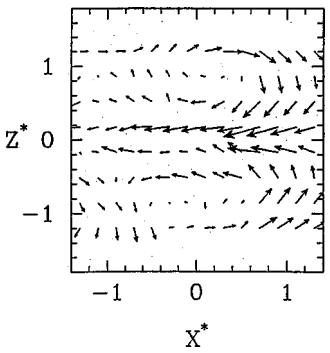

FIG. 11. Prediction of an instantaneous vector map from an idealized and scaled double roller template.

Figure 10 shows the point to point forecasting from a template of the double roller depicted in Fig. 7(a), properly scaled to match the rms values of the fluctuating field considered. This is necessary because the neural system has learned from real examples containing both large-scale and small-scale motions, i.e., from signals of a given amplitude. The predicted velocity map given in Fig. 10 corresponds to a double roller structure centered at $x^*=0$ and with an upstream saddle point at approximately $x^*=-1.2$. The observed randomness is due to the fact that the neural system was trained with turbulent flow data and has learned this randomness (see Fig. 3 of the auto-spectra).

To support the significance of this finding, several tests of point-to-point forecasting were carried out with input templates of unrealistic or highly improbable vector maps. The results showed that the neural system did not yield any plausible coherent topology or yield vector maps consistent with the space–time correlation of the data. Note that the velocity vector map of the double roller in Fig. 7(a) which has been used to generate Fig. 10 does not belong to the training set.

The final test for double rollers is the prediction of an instantaneous vector map of 10 velocity vectors from a properly scaled input vector containing the four instants of information located at $0.8 \leqslant x^* \leqslant 1.4$ in Fig. 7(a). In this case, the neural system predicts the double roller vector map of Fig. 11. There is agreement between the experimental and predicted structures, with the predicted one being slightly smaller in the streamwise direction of the flow. This is probably caused by the difficulty of learning and predicting a three-dimensional phenomena related with the occurrence of ring-shaped vortices[19] from only two-dimensional information and the fact that the neural system produces a slightly shorter auto-correlation than the experiments (see, e.g., Fig. 4). Nevertheless, the remarkable agreement between the double roller structure present in the laboratory data and in the vector map produced by the eight neural, indicates the potential of the proposed cognitive system to capture the dynamics of turbulent flows and be utilized as an expert system. Note that differences in the modulus of the vector plots in both figures are caused by the scaling of the input signal.

B. New observed structural features in the far wake

One of the things that has puzzled us is the lack of symmetry around the saddle points in Figs. 8(a) and 8(b). Figure 8(a) shows a double roller just downstream of the saddle point and a large roller (which hints at being a large double roller). There appears to be flow directly from the center of the double roller to the top of the upstream counterclockwise roller. Large single rollers were first found by Mumford[12] and later by Ferré and Giralt.[13] Ferré and Giralt found that when a large single roller (i.e., larger than either roller making up the double roller structure) was identified there was also evidence that it was simply a portion of a larger double roller structure. Since then, no one has investigated the dynamics of these large single rollers, although the double roller structure has been extensively investigated, most recently by Vernet *et al.*[19]

The first step in this process was to determine whether the neural system had learned of the existence of the large single rollers. To do this, the type of simulation we performed to generate Fig. 11 was repeated. The results are shown in Fig. 12. However, in Fig. 12 the four right-most

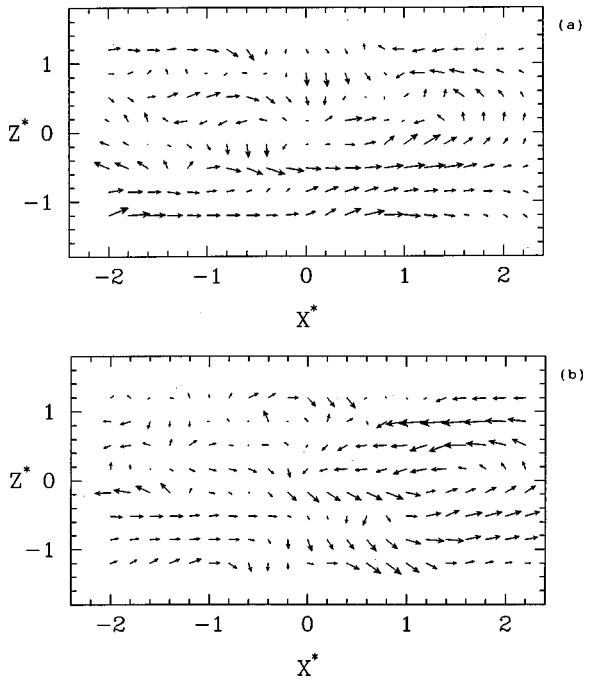

FIG. 12. Prediction of an instantaneous vector map from an indealized large scale roller template for two different initial conditions of the velocity field. The initial condition is shown by the four rightmost vectors in (a) and (b).

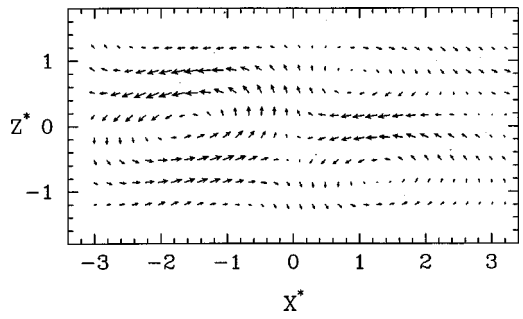

FIG. 13. A pattern recognition analysis of the double roller—saddle—large single roller configuration present in the experimental velocity data.

data points are the historical data given to the neural system as input. The given historical time data in Fig. 12 is characterized by the upstream portion of a saddle point [such as that given in Fig. 12(a)] in the lower four probes and negative spanwise velocity fluctuations in the probes $0 \leqslant z^* \leqslant 1$. A large scale counterclockwise motion can be seen to extend an additional eight time points (for a total of 12, which is approximately $2l_0$). Beginning with a slightly different pattern, more like a vortex, a large single roller structure is clearly observed in Fig. 12(b). Thus, it is clear that the neural system has learned about these large single rollers.

The pattern recognition technique of Ferré and Giralt[13] also finds this configuration in the experimental data, as shown in Fig. 13. However, finding such a pattern requires a detailed knowledge about the ordering of the structures, which one cannot normally infer in advance. Figure 13 shows a large counterclockwise roller immediately upstream of the double roller structure. About 1/3 of the events contributing to the double roller structure of Fig. 7(a) are immediately followed by a large single roller like the one depicted in Fig. 13. A similar proportion is found for the symmetrical configuration, i.e., when the large single roller rotates clockwise. Interestingly, the upstream saddle point still exists without the symmetry of two adjacent double rollers (of opposite sense). Actually, this is not unlike a vertical shear plane in the near region of a two-dimensional vortex shedding object. In this latter case, saddle points are also surrounded by three adjacent foci (or rollers). To see this in the present work, the plot needs to be rotated about 45°.

When Fig. 13 is added to the opposite symmetric pattern, i.e., that with an upstream clockwise vortex, the result is the double roller pattern of Fig. 7(a). Thus, the pattern recognition technique[13] could not educe these additional features of the data because the adjacent structures are randomly aligned in different orientations. However, these larger single roller patterns, with clockwise and counterclockwise rotation, are a significant feature of the flow since they follow the individual double roller events in 2/3 of the cases.

The origins of this ordering of patterns is likely due to the arrangement of adjacent Kármán vortices and rib structures as they bend and kink in the near region (e.g., Kiya and Matsumura[35]). This will be the subject of a future investigation.

V. CONCLUSIONS

The present results indicate that the proposed neural system is capable of capturing the highly nonlinear dynamics of free turbulence. Synthetic signals were generated with the fuzzy ARTMAP network at eight different positions in the homogeneous plane of cylinder wake. Spectral analysis, POD, and pattern recognition were used to show that the simulated signals capture the main features of the turbulence.

The present neural network was also applied as an interactive expert system to recognize the individual classes of events present in complex shear flows. Idealized velocity signals (patterns) are input to the network and a point-to-point forecast of the resulting velocities is performed. This allows hypotheses about the turbulence structure to be investigated. With this approach, large single roller structures are observed upstream of the well-known double roller structures, with a saddle point between them.

ACKNOWLEDGMENTS

We would like to thank Professor R. A. Antonia for providing his experimental data. This work was financially supported by the DGICYT project PB96-1011.

[1] A. A. Townsend, ''The structure of turbulent shear flow,'' 2nd ed. (Cambridge University Press, Cambridge, 1976).
[2] W. D. McComb, ''The physics of fluid turbulence'' (Oxford University Press, Oxford, 1990).
[3] M. Nelkin, ''In what sense is turbulence an unsolved problem?'' Science **255**, 566 (1992).
[4] L. P. Kadanoff, ''Turbulent excursions,'' Nature (London) **382**, 116 (1996).
[5] K. R. Sreenivasan, ''Turbulence and the tube,'' Nature (London) **344**, 192 (1990).
[6] G. L. Brown and A. Roshko, ''On density effects and large structures in turbulent mixing layers,'' J. Fluid Mech. **64**, 775 (1974).
[7] R. E. Falco, ''Coherent motion in the outer region of turbulent boundary layers,'' Phys. Fluids **20**, S124 (1977).
[8] H. L. Grant, ''The large eddies of turbulent motion,'' J. Fluid Mech. **4**, 149 (1958).
[9] J. L. Lumley, ''The structure of inhomogeneous turbulent flows,'' *Proceedings of the International Colloquium on Atmospheric Turbulence and Radio Wave Propagation*, (Moscow, 1965), pp. 166–176.
[10] R. J. Adrian and P. Moin, ''Stochastic estimation of organized turbulent structure: Homogeneous shear flow,'' J. Fluid Mech. **190**, 531 (1988).
[11] R. A. Antonia, ''Conditional sampling in turbulence measurements,'' Annu. Rev. Fluid Mech. **13**, 131 (1981).
[12] J. C. Mumford, ''The structure of the large eddies in fully developed turbulent shear flows. Part 2. The plane wake,'' J. Fluid Mech. **137**, 447 (1983).
[13] J. A. Ferre and F. Giralt, ''Pattern recognition analysis of the velocity field in plane turbulent wakes,'' J. Fluid Mech. **198**, 27 (1989).
[14] J. Ferre-Gine, R. Rallo, A. Arenas, and F. Giralt, ''Identification of coherent structures in turbulent shear flows with a Fuzzy ARTMAP neural network,'' Int. J. Neural Syst. **7(5)**, 559 (1996).
[15] G. A. Kopp, J. A. Ferre, and F. Giralt, ''The use of pattern recognition and Proper Orthogonal Decomposition in identifying the structure of fully-developed free turbulence,'' ASME J. Fluids Engineering **119**, 289 (1997).
[16] S. Banerjee, ''Turbulence structures,'' Chem. Eng. Sci. **47**, 1793 (1992).
[17] J. Zhou, R. J. Adrian, and S. Balachandar, ''Autogeneration of near-wall vortical structures in channel flow,'' Phys. Fluids **8**, 288 (1996).
[18] D. K. Bisset, R. A. Antonia, and L. W. B. Browne, ''Spatial organization of large structures in the turbulent far wake of a cylinder,'' J. Fluid Mech. **218**, 439 (1990).
[19] A. Vernet, G. A. Kopp, J. A. Ferre, and F. Giralt, ''Three-dimensional structure and momentum transfer in a turbulent cylinder wake,'' J. Fluid Mech. **394**, 303 (1999).

[20]G. A. Carpenter, S. Grossberg, N. Marcuzon, J. H. Reinolds, and D. B. Rosen, ''Fuzzy ARTMAP: A neural network architecture for incremental supervised learning of analog multidimensional maps,'' IEEE Trans. Neural Netw. **3**, 698 (1992).
[21]J. Denker, D. Schwartz, B. Wittner, S. Solla, R. Howard, L. Jackel, and J. J. Hopfield, ''Large automatic learning, rule extraction and generalization,'' Complex Syst. **1**, 877 (1987).
[22]H. S. Seung, H. Sompolinsky, and N. Tishby, ''Statistical mechanics of learning from examples,'' Phys. Rev. A **45**, 6056 (1992).
[23]A. Tzes and J. Borowiec, ''Applications of fuzzy logic and neural networks to identification and control problems in fluid mechanics,'' *Proceedings of ASME Fluids Engineering Division*, (FED-242, 1996), pp. 29–34.
[24]M. Lee, J. Kim, D. Babcock, and R. Goodman, ''Application of neural networks to turbulence control for drag reduction,'' Phys. Fluids **9**, 1740 (1997).
[25]G. A. Carpenter and S. Grossberg, ''A massively parallel architecture for a self-organizing pattern recognition machine,'' Comput. Vis. Graph. Image Process. **37**, 54 (1987).
[26]G. A. Carpenter, and S. Grossberg, and J. H. Reynolds, ''ARTMAP: Supervised real-time learning and classification of nonstationary data by a self-organizing neural network,'' Neural Networks **4**, 565 (1991).
[27]G. A. Carpenter, and S. Grossberg, and D. Rosen, ''Fuzzy ART: Fast stable learning and categorization of analog patterns by an adaptative resonance system,'' Neural Networks **4**, 759 (1991).
[28]R. Kühn, J. L. van Hemmen, and U. Riedel, ''Complex temporal association in neural networks,'' J. Phys. A **22(15)**, 3123 (1989).
[29]B. Kosko, *Neural Networks and Fuzzy Systems* (Prentice Hall, Englewood Cliffs, 1992), pp. 189–219.
[30]L. Zadeh, ''Fuzzy sets,'' Inf. Control. **8**, 338 (1965).
[31]F. Takens, ''Detecting strange attractors in turbulence, Dynamical systems and turbulence,'' Lect. Notes Math. **898**, 366 (1981).
[32]A. Scotti, C. Meneveau, and S. G. Saddoughi, ''Fractal dimension of velocity signals in high Reynolds-number hydrodynamic turbulence,'' Phys. Rev. E **51**, 5594 (1995).
[33]J. Kim, P. Moin, and R. J. Moser, ''Turbulence statistics in fully developed channel flow at low Reynolds number,'' J. Fluid Mech. **177**, 133 (1987).
[34]F. R. Payne and J. L. Lumley, ''Large eddy structure of the turbulent wake behind a circular cylinder,'' Phys. Fluids **10**, S194 (1967).
[35]M. Kiya and M. Matsumura, ''Incoherent turbulence structure in the near wake of a normal plate,'' J. Fluid Mech. **190**, 343 (1988).